FINAL REPORT

NASA Langley Cooperative Agreement NCC-1-266

Development of a Design Methodology for Reconfigurable Flight Control Systems

Report Text Title: Accommodating Actuator Failures in Flight Control Systems

Ronald A. Hess
Dept. of Mechanical and Aeronautical Engineering
One Shields Ave.
University of California
Davis, CA 95616-5294
(530)-752-1513
rahess@ucdavis.edu

ACCOMMODATING ACTUATOR FAILURES IN FLIGHT CONTROL SYSTEMS

R. A. Hess[1], W. Siwakosit[2] and J. Chung[3]
Dept. of Mechanical and Aeronautical Engineering
University of California
Davis, CA 95616

Abstract

A technique for the design of flight control systems that can accommodate a set of actuator failures is presented. As employed herein, an actuator *failure* is defined as any change in the parametric model of the actuator which can adversely affect actuator performance. The technique is based upon the formulation of a fixed feedback topology which ensures at least stability in the presence of the failures in the set. The fixed compensation is obtained from a loop-shaping design procedure similar to Quantitative Feedback Theory and provides stability robustness in the presence of uncertainty in the vehicle dynamics caused by the failures. System adaptation to improve performance after actuator failure(s) occurs through a static gain adjustment in the compensator followed by modification of the system prefilter. Precise identification of the vehicle dynamics is unnecessary. Application to a single-input, single-output design using a simplified model of the longitudinal dynamics of the NASA High Angle of Attack Research Vehicle is discussed. Non-real time simulations of the system including a model of the pilot demonstrate the effectiveness and limitations of the approach.

---

[1]Professor and Vice Chairman, Associate Fellow, AIAA

[2]Graduate Student

[3]Postdoctoral Researcher

Introduction

The requirements that will accompany the design of future, high-performance aircraft, whether inhabited or uninhabited, will likely include some ability to automatically reconfigure the aircraft flight control system to accommodate control effector failure(s) and/or damage to the airframe itself. The advent of Uninhabited Combat Air Vehicles (UCAV's)[1] will certainly increase research activity in this area, as will recent emphasis on airline safety.[2] Thus, the design of "reconfigurable" or "restructurable" flight control systems is of continuing importance to the research community. Reconfigurable control systems are those possessing the ability to accommodate system failures automatically through on-line self-modification. Reconfigurable control is a challenging design problem, as it usually entails failure-detection, system identification, and on-line controller-redesign. A sampling of this research can be found in Refs. 3-12.

The design philosophy to be discussed herein will be applied to the problem of failure of one or more of the actuators which drive the thrust/aerodynamic effectors in a flight control system, e.g., elevator, thrust-vectoring nozzles. Attention will be focused upon maintaining stability and performance in the presences of these failures. The flight control scenario to be examined assumes that the human pilot is controlling the vehicle when failure occurs, and will resume control after reconfiguration is completed. While actuator failures constitute only a subset of possible damage that can occur to a flight vehicle, the ability to accommodate such damage in a flight control system is pertinent for the following reason: The control effectors which the actuators drive are powerful force and moment producers. Thus, if a design methodology can provide stability and performance robustness in the presence of failure of these devices, there is reasonable hope that it can serve as a candidate reconfigurable design methodology for other classes of problems, e.g., airframe damage.

Conceptually, the design approach to be discussed is considerably less complex (and admittedly less mathematically sophisticated) than others which have been proposed, e.g., Refs. 3-12, in that much of the flight control system remains unchanged in the presence of the actuator failure. This design philosophy was pursued for simplicity and for its reliance upon proven frequency-domain design techniques. It may be hyperbole to refer to the adaptive formulation employed here as a "reconfigurable" control system, however, for the sake of brevity, this will be done.

Approach

Design Preliminary Considerations

The research to be described will first concentrate upon ensuring that the aircraft Stability and Command Augmentation System (SCAS) is as robust as possible to the effects of actuator failure(s). This implies requiring at least stability in the presence of the failures to be considered and will depend upon the existence of redundant aerodynamic/propulsive control effectors, i.e., effectors that provide control authority comparable to that of the effector(s) whose actuator(s) has failed. While the existence of redundant effectors may seem to be a significant requirement, it must be emphasized that the reconfiguration technique being discussed is intended to accommodate *complete* as well as partial failure of actuators. An important part of the design procedure for the undamaged aircraft is the inclusion of software rate limiters, whose purpose is to improve system performance when actuator saturation occurs. The design and utility of such software rate limiters have been discussed in the literature.[13]

Design Philosophy

The philosophy behind the design approach rests upon the established tenet that careful application of frequency-domain loop-shaping techniques can provide a SCAS (with fixed compensator) which exhibits stability and performance robustness in the presence of significant

uncertainty in the dynamics of the vehicle being controlled. An attempt to extend this approach to encompass uncertainty brought about by actuator failures would likely produce compensators with unacceptably high bandwidth. However, reducing the requirements on the compensator to providing stability and performance robustness for the undamaged vehicle and only stability robustness for the damaged vehicle can offer a significant reduction in required system bandwidth. Creating an adaptive system with a modest amount of reconfiguration capability would allow some of the performance robustness, lost in the failures, to be regained. Thus, the approach to be discussed will distribute the responsibility for accommodating actuator failures between a fixed compensation element or elements and a relatively simple adaptive system.

Design Framework

Figure 1 is a diagrammatic representation of the design framework to be pursued. Note that full-envelope design is the goal. One begins with a set of healthy aircraft models, i.e., those with undamaged actuators, at the flight conditions representative of the vehicle's operational envelope. To this set is appended the failed aircraft models, i.e., those with damaged actuators. Performance goals for the healthy aircraft are established that ensure satisfactory handling qualities with no tendencies for pilot-induced oscillations. Analytical means addressing these latter design constraints are available.[14] Failure detection will *not* be addressed in what follows. It will be assumed that the failure of an actuator(s) will be detected, but that the nature of this failure and the particular actuator(s) involved will not be known.

Pre-Design Technique A QFT Pre-Design Technique (PDT)[15] is employed and flight control laws (compensation elements) are created with the PDT that attempt to (1) meet the performance goals for the undamaged aircraft, (2) ensure stability for the damaged aircraft, and to (3) minimize the necessity of *dynamic* reconfiguration, i.e., that requiring changes in the dynamic compensation elements of the SCAS. The possibility of gain-scheduling with flight

condition is included with the aim of reducing controller bandwidths. Finally, and if necessary, a "formal" QFT design can be undertaken in which the approximate control laws obtained with the PDT are evaluated and modified, if necessary.[15] It is important to note that, as with any QFT design, stability can be guaranteed not just for those failures which are explicitly included in the failed set, but for any failures that exhibit dynamics with magnitude and phase characteristics that fall within the bounds defined by the members of the original failure set. This will be demonstrated in the example to be considered.

Adaptive Logic While the final QFT design will ensure satisfactory handling qualities and PIO immunity for the healthy aircraft, only stability will be sought with the damaged aircraft. Hence, an adaptive system is created for the purpose of recovering as much performance as possible under conditions of actuator failure. Concentrating upon a single-input, single-output (SISO) system (or a single loop of a multi-input, multi-output system) for the purposes of exposition, the adaptive logic consists of two parts. The first part is simply a static gain that multiplies the compensator obtained from the PDT approach (which emulates a QFT design). The multiplicative term is adjusted based upon the system response to a test input. The ability of a single, variable gain to ensure stability is a result of the PDT approach. The second part of the logic involves a reconfiguration of the SCAS prefilter as a lead-lag element with parameters also dependent upon the system response to the test input. This reconfiguration recoups SCAS bandwidth lost when stability is maintained through the static gain variation just described.

The adaptive logic is implemented as follows: After detection of a failure, a test square-wave input is applied to the SCAS (with pilot inputs eliminated). A simple classification technique is employed in which responses are first characterized as oscillatory ("positive" overshoot) and non-oscillatory ("negative" overshoot, i.e., no overshoot and sluggish response).

Based upon this classification, the static gain term is varied until the responses meet a percent overshoot (PO) criterion, e.g., $PO_{min} \leq PO \leq PO_{max}$. The time from the initiation of each pulse of the square-wave to the response variable's achieving it maximum value is used determine the form of the prefilter lead term. As just described, the "reconfiguration" formulation appears very ad-hoc in nature. However, it is based upon relatively simple, time and frequency-domain relationships which can be examined in real-time as part of the adaptive logic.

Simulation Non-real time and piloted simulation complete the design process outlined in Fig. 1. In the former simulation category, realistic models of pilot tracking behavior should be included.

An Example

Design Overview

Pre-Design Technique A brief example of a SISO system can be offered that demonstrates the design procedure. Figure 2 shows the former NASA High-Angle-of-Attack Research Vehicle (HARV). For the purposes of this example, attention is focused on longitudinal pitch-control with redundant effectors consisting of the elevator (stabilator) and pitch-thrust vectoring. For brevity's sake, only a single flight condition is employed here. Thus, the performance bounds one finds in a typical QFT design are not employed. Figure 3 shows the pitch-rate flight control system diagram and pilot-loop closure for pitch-attitude tracking.

The Pre-Design Technique can be briefly summarized as follows. The compensator $G_c(s)$ is chosen as

$$G_c(s) = \frac{\omega_c}{s} \cdot \frac{1}{\frac{q}{u_c}|_{nom} \cdot (\frac{s}{15\omega_c} + 1)^p} \qquad (1)$$

where ω_c is the crossover frequency of the SCAS loop transmission $\frac{q}{q_e}$

$\frac{q}{u_c}|_{nom}$ is the q to u_c transfer function for the undamaged vehicle

p is the excess of poles over zeros in $\frac{q}{u_c}|_{nom}$

The minimum crossover frequency is the found for which (a) the variation in $\left|\frac{q}{q_c}(j\omega)\right|$ is satisfactory for the undamaged vehicle given uncertainty introduced by considering different flight conditions and/or by errors in the vehicle model, (b) rejection of constant disturbances injected as the actuator inputs is minimized, i.e. to minimize effects of non-zero null failures of the actuators, and (c) $\frac{q}{q_c}$ is stable for all actuator failures considered. Prefilter dynamics $F(s)$ are then selected to yield predicted level one handling qualities with no PIO susceptibility for the undamaged vehicle. Care must obviously be taken in employing Eq. 1 if $\frac{q}{u_c}|_{nom}$ is unstable or possesses right-half plane zeros (neither of which occurred in this example). In the former case, ω_c must be greater than the real part of the unstable pole with the most positive real part, and pole-zero cancellation with the plant must be avoided, while in the latter case, ω_c must be less than the real part of the non-minimum phase zero with the most positive real part, and again, pole-zero cancellation with the plant must be avoided.

Table 1 gives the vehicle and (healthy) actuator dynamics, taken from Ref. 16. In addition, characteristics of the cockpit force/feel system, to be included in the pilot/vehicle simulation are given. Also note that rate and amplitude-limiting were included in the actuator models. Table 2 lists the actuator failure characteristics. A set of 35 combinations of actuator failures define the damaged vehicle set. This set includes the undamaged or healthy aircraft.

Figure 4 shows the bode diagrams of the transfer functions q/u_c from Fig. 3 with the 35 failures. Compensation and prefilter elements $G_q(s)$ and $F(s)$ were obtained using the PDT of Ref. 15 ensuring that the criteria described in the preceding were satisfied, i.e., predicted level one handling qualities and no predicted PIO tendencies with the undamaged aircraft, stability with the damaged aircraft, with the potential of crossover-frequency variation (through a multiplicative gain) stabilizing the SCAS. The handling and PIO predictions were accomplished using the pilot modeling procedure described in Ref. 17. The resulting $G_c(s)$, $F(s)$ and ω_c were

$$G_c(s) = \frac{-20.2(s^2+2(0.35)1.12s+1.12^2)(s^2+2(0.6)20s+20^2)(s^2+2(0.69)30s+30^2)}{s(s+0.493)(s^2+2(0.606)21.14s+21.14^2)(s+37.5)^3}$$

$$F(s) = \frac{0.3s+1}{0.1s+1} \qquad (2)$$

$$\omega_c = 2.5 \ rad/\text{sec}$$

The complexity of $G_c(s)$ is dut to the PDT which involves inversion of the plant dynamics (including actuators) as indicated in Eq. 1. Simplification of $G_c(s)$ is possible, but was not pursued herein. Figure 5 shows the Bode diagram of $G_c(s)$. Since $|G_c(j\omega)|$ does not increase beyond the 2.5 rad/sec crossover frequency, a modest "cost of feedback" is involved.[15]

Software Rate Limiters and Control Distribution Matrix The software rate limiters will be discussed only briefly herein. These devices have shown promise for improving the performance in the presence of actuator saturation under normal operation[13] and have thus been included as part of the SCAS design. For their implementation the software limiters require a control distribution matrix $\boldsymbol{K}$ which distributes the single pseudo-control u_c to the two actuators, one commanding stabilator position and the second commanding pitch thrust nozzle position. For rate limiter implementation, each row of $\boldsymbol{K}$ contains only a single non-zero entry equal (or proportional) to the magnitude of the rate-limit of the actuator which it affects. In the relatively

simple example here, $\boldsymbol{K}$ is thus chosen as

$$\boldsymbol{K} = \begin{bmatrix} 1 \\ 1 \end{bmatrix} \tag{3}$$

The software limiters are implemented so that the maximum *rate* command to either actuator does not exceed its rate limit, here 60 deg/sec for either actuator as indicated in Table 1. Note that the differentiating "s" in Fig. 3 is always subsumed into the strictly proper $G_c(s)$.

Fixed Compensation Figure 6 shows the SCAS loop transmissions (q/q_e in Fig. 3) for the 35 failures on a Nichols chart. Note that closed-loop stability is in evidence. For comparison, Fig. 7 is a similar diagram for the undamaged aircraft. Figure 8 demonstrates the extreme variation in closed-loop behavior of the SCAS which occurs with failed actuators. Here, the SCAS step responses (q to q_{cp} from Fig. 3) for all the failure cases are shown. By contrast, Fig. 9 shows the step response for the undamaged aircraft.

Adaptive Logic As alluded to in the preceding, the adaptive logic which defined the reconfigurable system was predicated upon real-time examination of the pitch-rate response $q(t)$ to a square-wave command injected as shown in Fig. 3, with pilot inputs excluded from the system. Based upon the bandwidths of q/q_c for the failed systems with the fixed compensation of Eq. 2, the duration of each pulse of the square wave was selected as 4 sec, with the first 2 sec of the response to each pulse examined in the adaptive system. The static multiplying term included in $G_c(s)$ was $(1 + K_D)$ where K_D was initially zero. K_D was then varied in the following manner: If the response to the square-wave pulse indicated "negative" overshoot (i.e., no overshoot and a value less than the commanded value two sec from the initiation of any square-wave pulse) then K_D was increased. If the response indicated an overshoot, K_D was decreased. The adaptive logic was such that changes in K_D were inversely proportional to the amount of overshoot (positive or negative), i.e.,

$$K_D(0) = \pm 0.1$$

$$K_{D_1}(kT) = K_D((k-1)T) \pm \frac{1}{|0.05 \cdot PO|} \tag{4}$$

$$K_d(kT) = \pm \min[\,|K_{D_1}(kT)|,\ 1.2 \cdot |K_D((k-1)T)|\,]$$

with the "+" or "-" sign depedent upon whether a "positive" or "negative" overshoot was in evidence. Equation 4 implies that after the initial 0.1 value, changes in K_D were relatively small early in the adaptive procedure. This was done for the following reason: It is possible that large turbulence disturbances could mask the nature of the q-step response of the vehicle. Thus, an K_D change of incorrect sign could occur early in the adaptation. If this incorrect change were large enough, the SCAS could be destabilized. The overshoot criterion which determined whether reconfiguration was to be initiated, and if initiated, when it should be terminated was

$$-5\% \leq PO \leq 10\% \tag{5}$$

Selection of PO_{max} and PO_{min} was based upon the desire to allow K_D variation to provide most of the transient response improvement for the SCAS.

The prefilter reconfiguration was employed to improve the transient response characteristics of q/q_{cp} beyond that obtainable with variation in the SCAS compensator gain $(1+K_D)$, alone. It involved first removing the prefilter of Eq. 2 when a failure had been detected, i.e. setting $F(s) = 1.0$. After the final K_D value had been obtained, a new prefilter was inserted in the system, given by

$$F'(s) = \frac{[(T_M/4)s+1]^2}{(0.1s+1)^2} \tag{6}$$

where T_M is the "effective" time constant of the q response. The $F'(s)$ given by Eq. 6 implies amplification of the pilot's command in the frequency range beyond $4/T_M$. This amplification

is attributable to the severe nature of the failures in the modeled set, many of which introduced large, serial, time delays in the SCAS. Thus the characteristics of $F'(s)$ are a necessary part of the price to be paid for reconfiguration with the present scheme. It should be emphasized, that the impact of this amplification will be a function of q/q_c with failed actuators. In Eq. 6, T_M was the time at which the response variable q achieved its maximum value within the duration of any pulse of the square-wave input, (or 2 sec, whichever was smaller). This T_M definition is shown in Fig. 10 for the "positive" and "negative" overshoot cases just described. Equation 6 was obtained by first approximating the bandwidth ω_B of q/q_c as

$$\omega_B \approx \frac{4}{T_M} \tag{7}$$

Two simple zeros for the prefilter $F'(s)$ were then placed at $s = -\omega_B$.

Simulation

Pilot Model The efficacy of the design technique just outlined was investigated in a non-real time simulation. A realistic pilot model was included[17] with dynamics based upon the undamaged vehicle. A cross-over frequency of 1.5 rad/sec was selected as representing aggressive tracking behavior. The pilot model took the form

$$Y_p(s) = \frac{2.5 \cdot 10^5 \cdot e^{-0.2s}}{[0.146,14.1][0.778,28.9]} \tag{8}$$

After reconfiguration, the pilot model gain was adjusted so as to maintain the original 1.5 rad/sec crossover frequency. This is equivalent to limiting pilot adaptation to the reconfigured dynamics (or damaged dynamics in the case where no reconfiguration is allowed) to a change in "gain". In practice, it would be advisable to reduce the prefilter gain (say by 50%) as part of the reconfiguration so as to minimize the possibility of PIO tendencies. Gain reductions such as this have been linked to the elimination of PIO's in some pilot-in-the-loop simulations.[18]

Tracking Task The pitch-attitude tracking task of Fig. 3 was simulated wherein the pilot closed a pitch-attitude loop, with q_{cp} serving as the pilot command to the SCAS. A pseudo-random sum of sinusoids provided the tracking command θ_c. The root-mean-square value of this command was 5.7 (0.1 rad) deg. In addition, turbulence was included in the simulation by injecting a random pitch-rate disturbance with an RMS value of 0.57 deg/sec (.01 rad/sec) into the vehicle pitch-rate response. During reconfiguration, no pilot inputs were allowed. After reconfiguration, the pilot model resumed tracking the sum-of sinusoids command as just described.

Simulation Examples System performance was evaluated for each of the 35 failures. Space permits only a discussion of two of the most extreme cases. First, Fig. 11 shows the pilot/vehicle tracking performance for the undamaged vehicle. Figure 12 shows the performance after reconfiguration for a failure in which the thrust nozzle actuator fails completely (in the null position) and the stabilator actuator suffers a 50% reduction in effectiveness or steady-state gain. Figure 13 shows the performance without reconfiguration. As mentioned previously, when no reconfiguration was allowed, the pilot/vehicle crossover frequency was still adjusted to maintain the 1.5 rad/sec crossover frequency after failure. This permitted a fair comparison with the tracking performance when reconfiguration was allowed. Figure 14 shows the pilot/vehicle tracking performance following a failure in which the thrust nozzle actuator has again failed completely and the stabilator actuator has a damaged-induced 0.2 sec added time delay. In this case, when no reconfiguration was allowed the pilot/vehicle system was unstable. Before reconfiguration for the two cases just presented, the q to q_c responses of the damaged vehicles were sluggish and highly oscillatory, respectively. Figure 15 shows the reconfiguration responses for the failure of Fig. 12. i.e., the vehicle's pitch-rate response to the square-wave pitch-rate inputs as the adaptive logic changes K_D to achieve the desired percent overshoot. Figure 16 shows the corresponding increments in, and final value for, K_D. Figures 17 and 18

show similar results for the failure of Fig. 14. In the reconfigurations for these two failures, T_M in Eq. 6 was 0.5 sec. In the first of the reconfigurations the elapsed time from beginning to end of reconfiguration until the final K_D value was obtained was 12 sec, while for the second, the time was 36 sec. The average reconfiguration time for all 35 configurations was 25.2 sec, with the longest being 68 sec. This average did not included those cases (11 in number) for which no reconfiguration was necessary, i.e., the damaged vehicle was found to meet the overshoot requirements of Inequality 4. Performance was always found to improve with the adaptive system when reconfiguration was found to be necessary.

Of interest is the simulation of a failure that was *not* a member of the modeled set. As mentioned in the preceding, the only constraint here is that the diagram of the loop transmission $\frac{q}{q_e}$ of the unmodeled failure must lie within the bounds of the loop transmissions of all of the modeled cases on the Nichols chart. The Nichols chart of Figure 19 shows one such unmodeled failure that meets this criterion. In this failure the thrust nozzle actuator fails completely, the steady-state gain of the stabilator actuator increases by 50% and the undamped natural frequency of the actuator is reduced from 30 rad/sec to 10 rad/sec. Figure 20 shows the tracking performance of the pilot/vehicle system with this failure. In this instance, the criterion of Inequality 4 was met *without* reconfiguration, so the SCAS and prefilter dynamics remain unchanged. The tracking performance is seen to be quite satisfactory.

Finally, an additional failure similar to one in the modeled set was included which involved a complete elevator actuator failure with a non-null angle of 5 deg was evaluated. Again the reconfiguration scheme performed well. This performance was ensured in the PDT by requiring good low-frequency disturbance rejection properties for disturbances injected in parallel with the signal u_c in Fig. 3. No significant actuator rate or amplitude saturation occurred during any of the failures. This leads quite naturally to the subject of the next section.

Utility of Software Rate Limiters Since the software rate limiters have been included in the design methodology, and since no significant rate limiting occurred in the 35 failure configurations simulated, a simulation involving artificially low actuator rate limits was conducted. These limits of 10 deg/sec on each of the actuators were considered to be the characteristics of healthy, undamaged actuators. One of the failure modes considered previously was again simulated, i.e., the thrust actuator failing completely and the stabilator actuator with 50% effectiveness. For the purpose of exposition, the pilot/vehicle response to a step pitch command rather than the sum of sinusoids was investigated after reconfiguration had occurred. Figure 21 shows the response of the undamaged system, and Fig. 22 shows the corresponding stabilator *rate*. Figure 23 shows the response of the damaged system after reconfiguration. Here $K_D = 0.743$, $T_M = 2.0$ sec, and the elapsed time from beginning to end of reconfiguration was 44 sec. Figure 24 shows the corresponding stabilator rate. Finally, Figs. 25 and 26 show corresponding results for the case in which no reconfiguration was allowed. Note the improved performance with reconfiguration. As in the previous examples, the pilot "gain" was adjusted to yield a 1.5 rad/sec crossover frequency after failures. The caveat here, however, is that this gain adjustment was made on the *linear* system, i.e., where rate limiting was absent. It should be noted that when the software rate limiters were removed in the reconfigurable design the pilot/vehicle system was unstable after reconfiguration. Thus, the inclusion of the software limiters is important. Finally, the increased "saturation" evident when reconfiguration was allowed is not saturation in the normal sense, i.e., the actuator is merely being driven by the software limiter up to its maximum rate, and no more.[13]

Discussion

The relative long adaptation times with a number of the failures in which reconfiguration occurred deserves some comment. The adaptive logic for changing K_D is quite rudimentary and no attempt was made to improve the speed of convergence for this study. Although the

requirement of SCAS stability in the event of failure eliminates the necessity of very rapid reconfiguration, improvement is certainly warranted in this area and is currently being pursued. It should be noted, however, that SCAS performance is improving at each iteration of the adaptive logic. The process could be terminated prematurely by the pilot if he/she so desires. Finally, the longer adaptation times were typically associated with the most severe of the actuator failures, i.e, those in which pilot/vehicle instability resulted when no reconfiguration was undertaken.

The extension of the technique discussed herein to MIMO systems is straightforward in theory. Test inputs would be alternated between control loops in the MIMO application, with the obvious penalty being increased adaptation times. As mentioned in the preceding, one disadvantage of the methodology lies in the high frequency amplification of pilot inputs created by the reconfigured prefilter, $F'(s)$. The possibility of biodynamic feedback through the control effector is a concern in these cases[19], as is the possibility that the reconfigured prefilter may increase the deleterious effects of damaged actuators wherein the damage affects the rate limit of the device. Finally, although the reconfiguration scheme allows recapture of much of the performance lost through actuator failure, it is doubtful whether the methodology can provide level one handling qualities for all the failures in the cases which were modeled.

Conclusions

A technique for the design of flight control systems that can accommodate actuator failures has been introduced and demonstrated for a simple SISO example which included a model of the pilot. The impetus behind the research was the consideration of actuator failure, *ab initio*, in the design process. The approach utilized relatively simple, frequency and time-domain design, with emphasis upon QFT-like loop-shaping methodology. Precise system identification of the dynamics of the damaged vehicle was unnecessary. No attempt was made

to minimize the adaptation times after failure(s) and the simulation results clearly indicate that the adaptive logic will have to be refined in order to successfully apply the technique to multi-input, multi-output systems. Research is currently underway in this area.

Acknowledgement

This work was supported by a grant from NASA Langley Research Center. The grant technical manager is Dr. Barton Bacon.

References

[1]Fulghum, D. A., "Unmanned Strike Next for Military," "U.S. Industry Searches for Design Formulas," "Payload, Not Airframe, Drives UCAV Research," "Navy Wants UCAV's for Carrier Use," *Aviation Week and Space Technology,* June 2, 1997, pp. 46-55.

[2]Anon, "Aviation Safety and Pilot Control," Report of the Committee on the Effects of Aircraft-Pilot Coupling on Flight Safety," National Academy Press, Washington, DC, 1997.

[3]Ostroff, A. J., and Hueshcen, R. M., "Investigation of Control Law Reconfiguration to Accommodate a Control Element Failure on a Commercial Aircraft," Proceedings of the 1984 American Control Conference, San Diego, CA, June, 1984.

[4]Horowitz, I., "A Quantitative Inherent Reconfiguration Theory for a Class of Systems," *International Journal of Systems Science,* Vol. 16, No. 11, 1985, pp. 1377-1390.

[5]Eslinger, R. A., and Chandler, P. R., "Self-Repairing Flight Control System Program Overview," IEEE National Aerospace and Electronics Conference, 1988, pp. 504-511.

[6]Ochi, Y., and Kanai, K., "Design of Restructurable Flight Control Systems Using Feedback Linearization," *Journal of Guidance, Control, and Dynamics*, Vol. 14, No. 5, 1991, pp. 903-911.

[7]Ward, D. G. and Barron, R. L., "A Self-Designing Receding Horizon Optimal Flight Controller," Proceedings of the American Control Conference, Seattle, WA, June, 1995, pp. 3490-3494.

[8]Dhayagude, N., and Gao, Z., "Novel Approach to Reconfigurable Control Systems Design," *Journal of Guidance, Control, and Dynamics*, Vol., 19, No. 4, 1996, pp. 963-966.

[9]Kim, B. S., and Calise, A. J., "Nonlinear Flight Control Using Neural Networks," *Journal of Guidance, Control, and Dynamics*, Vol., 20, No. 1, 1997, pp. 26-33

[10]Keating, M. K., Pachter, M., and Houpis, C. H., "Fault Tolerant Flight Control System: QFT Design, *International Journal of Robust and Nonlinear Control,* Vol. 7., 1997 pp. 551-559.

[11]Heiges, M., "Reconfigurable Controls for Rotorcraft," *Journal of the American Helicopter Society,* Vol. 42, No., 3, 1997, pp. 254-263.

[12]Burken, J. J., and Burcham, F. W., Jr., "Flight-Test Results of Propulsion-Only Emergency Control System on MD-11 Airplane," *Journal of Guidance, Control, and Dynamics,* Vol. 20, No. 5, 1997, pp. 980-987.

[13]Hess, R. A. and Snell, S. A., "Flight Control System Design with Rate Saturating Actuators," *Journal of Guidance, Control and Dynamics*, Vol. 20, No. 1, 1997, pp. 90-96.

[14]Hess, R. A., "Unified Theory for Aircraft Handling Qualities and Adverse Aircraft-Pilot Coupling," *Journal of Guidance, Control, and Dynamics*, Vol. 20, No. 6, 1997, pp. 1141-1148.

[15]Henderson, D. K., and Hess, R. A., "Approximations for Quantitative Feedback Theory Designs," *Journal of Guidance, Control, and Dynamics*, Vol. 20, No. 4., 1997, pp. 828-830.

[16]Adams, R. J., Buffington, J. M., Sparks, A. G. Banda, S. S., "An Introduction to Multivariable Flight Control System Design," WL-TR-92-3110, Oct. 1992, Flight Dynamics Directorate, Wright-Patterson AFB, OH.

[17]Zeyada, Y., and Hess, R. A., "PVD_{NL} Pilot/Vehicle Dynamics $_{NonLinear}$ An Interactive Computer Program for Modeling the Human Pilot In Single-Axis Linear and Nonlinear Tracking Tasks," Dept. of Mechanical and Aeronautical Engineering, University of California, Davis, CA, 1998.

[18]Smith, R. H., "Predicting and Validating Fully-Developed PIO" AIAA Paper No. 94-3669, AIAA Guidance, Navigation and Control Conference, Aug. 1-3, 1994, Scottsdale, AZ.

[19]Gibson, J. C., and Hess, R. A., "Stick and Feel System Design," AGARD-AG-332, Advisory Group for Aerospace Research & Development, March 1997.

Table 1 Nominal Vehicle Model

Nominal Flight Condition: Alt. = 30,000 ft Mach No. = 0.6

$$\dot{x}(t) = Ax(t) + Bu(t)$$

$$x(t) = [\alpha(t) \quad q(t)]$$

α = *angle of attack, deg* $\qquad$ q = *pitch rate, deg/s*

δ_s = *stabilator angle, deg* $\qquad$ δ_t = *thrust vector angle, deg*

$$A = \begin{bmatrix} -0.5088 & 0.994 \\ -1.131 & -0.2804 \end{bmatrix} \quad B = \begin{bmatrix} -0.9277 & -0.01787 \\ -6.575 & -1.525 \end{bmatrix}$$

Actuator Descriptions

stabilator: $\dfrac{30^2}{s^2+42.4s+30^2}$ $\qquad$ *amplitude limit* = ±30 *deg* $\qquad$ *rate limit* = 60 *deg*/sec

thrust vector: $\dfrac{20^2}{s^2+24s+20^2}$ $\qquad$ *amplitude limit* = ±30 *deg* $\qquad$ *rate limit* = 60 *deg*/sec

Cockpit Force/Feel System Dynamics

$$\frac{25^2}{s^2+35s+25^2}$$

Table 2 Actuator Failure Models

stabilator:	$\frac{30^2}{s^2+42.4s+30^2} \cdot K_E e^{-\tau_E s}$	$0 \le K_E \le 1.0$	$0 \le \tau_E \le 0.4$ sec
thrust vector:	$\frac{20^2}{s^2+24s+20^2} \cdot K_T e^{-\tau_T s}$	$0 \le K_T \le 1.0$	$0 \le \tau_T \le 0.4$ sec

35 actuator failures created by varying K_E, K_T, τ_E, and τ_T

Figure Captions

Figure 1 A framework for reconfigurable flight control system design

Figure 2 The NASA High Angle of Attack Research Vehicle

Figure 3 Pitch-rate SCAS and pilot/vehicle system

Figure 4 Bode plots of transfer functions of vehicle + actuators with actuator failures

Figure 5 Bode plot of PDT compensator $G_c(s)$

Figure 6 Nichols chart plot of SCAS loop transmissions for damaged aircraft

Figure 7 Nichols chart plot of SCAS loop transmissions for undamaged aircraft

Figure 8 SCAS step responses (q to q_{cp}) for damaged aircraft

Figure 9 SCAS step response (q to q_{cp}) for undamaged aircraft

Figure 10 Definition of q-response "effective" time constant

Figure 11 Pilot/vehicle pitch-attitude tracking performance for undamaged aircraft

Figure 12 Pilot/vehicle pitch-attitude tracking performance for damaged aircraft after reconfiguration - thrust actuator failed completely, stabilator with 50% effectiveness

Figure 13 Pilot/vehicle pitch-attitude tracking performance for aircraft damaged as in Fig. 12 but no reconfiguration

Figure 14 Pilot/vehicle pitch-attitude tracking performance for damaged aircraft after reconfiguration - thrust actuator failed completely, stabilator with added 0.2 sec delay

Figure 15 Reconfiguration responses for aircraft damaged as in Fig. 12

Figure 16 K_D variation during reconfiguration of Fig. 12

Figure 17 Reconfiguration responses for aircraft damaged as in Fig. 14

Figure 18 K_D variation during reconfiguration of Fig. 14

Figure 19 Nichols chart plot of SCAS loop transmission for damaged aircraft not in modeled set

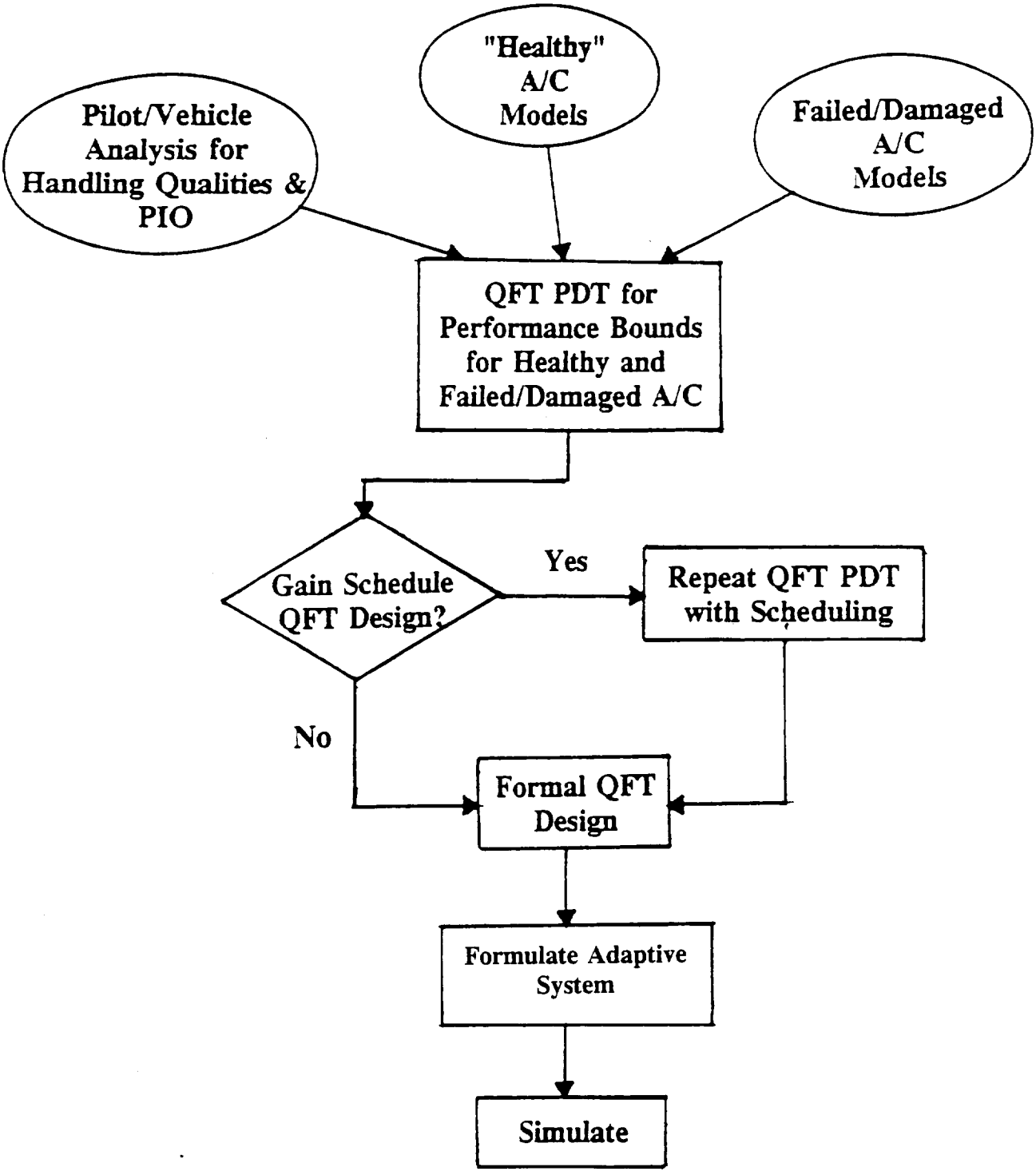

Figure 1 A Framework for Reconfigurable Flight Control System Design

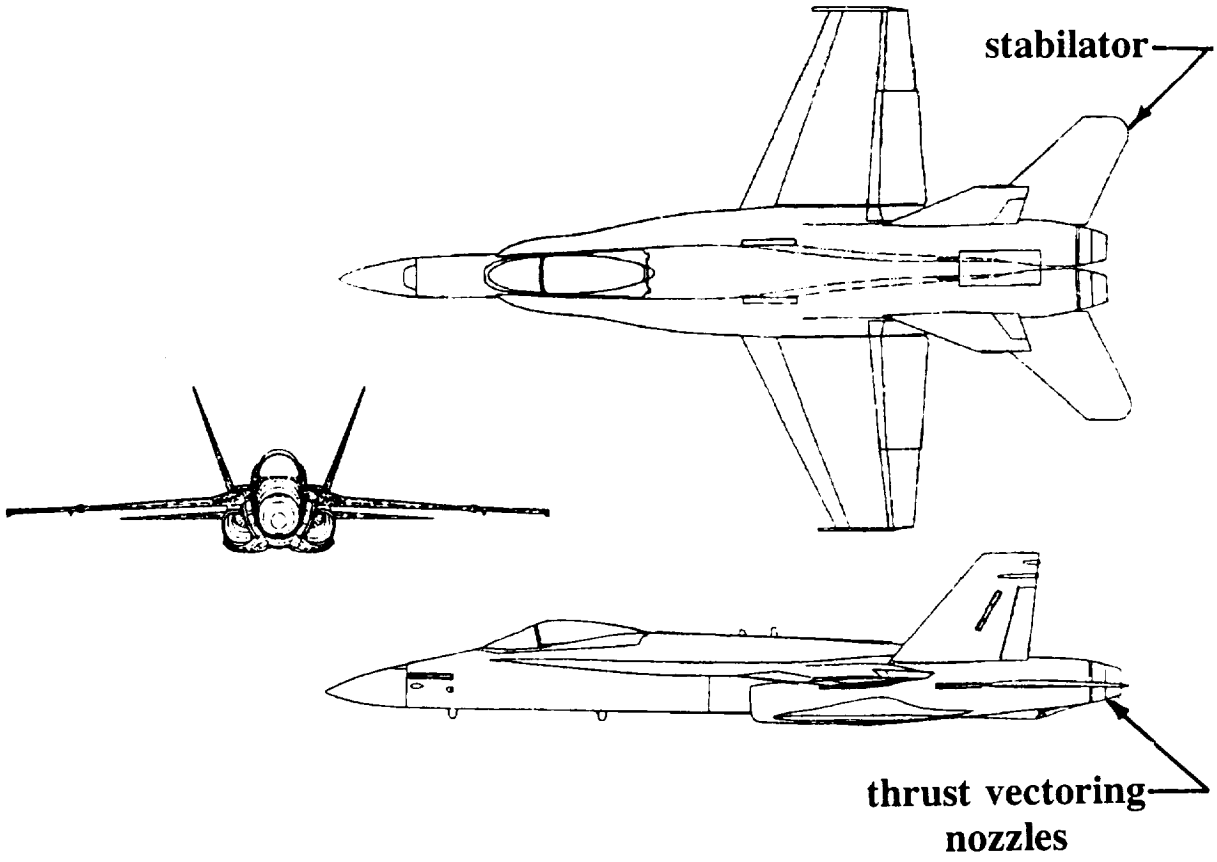

Figure 2 The NASA High Angle of Attack Research Vehicle

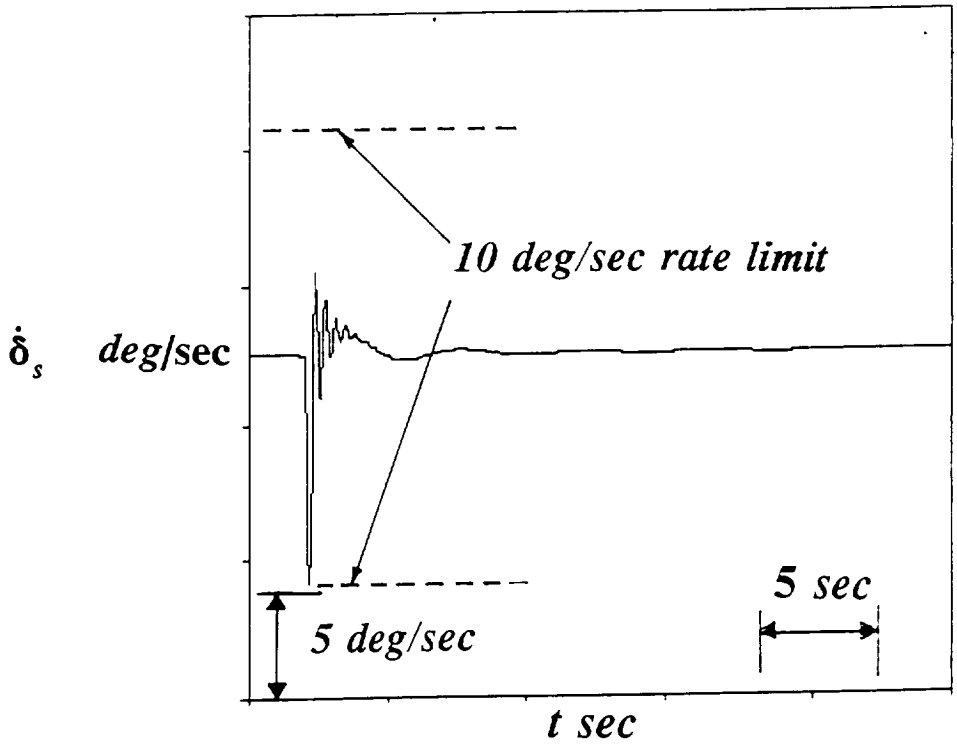

Figure 26 Stabilator rate corresponding to Fig. 25

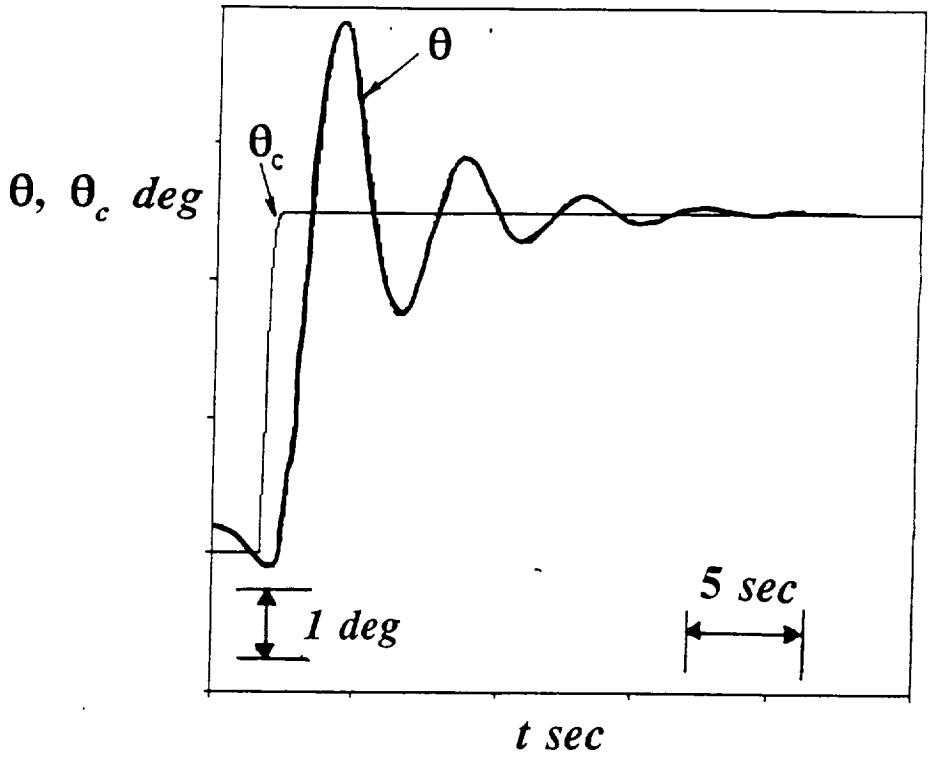

Figure 25 Pilot/vehicle pitch-attitude tracking performance for aircraft damaged as in Fig. 12, with actuator rate limiting of 10 deg/sec, no reconfiguration

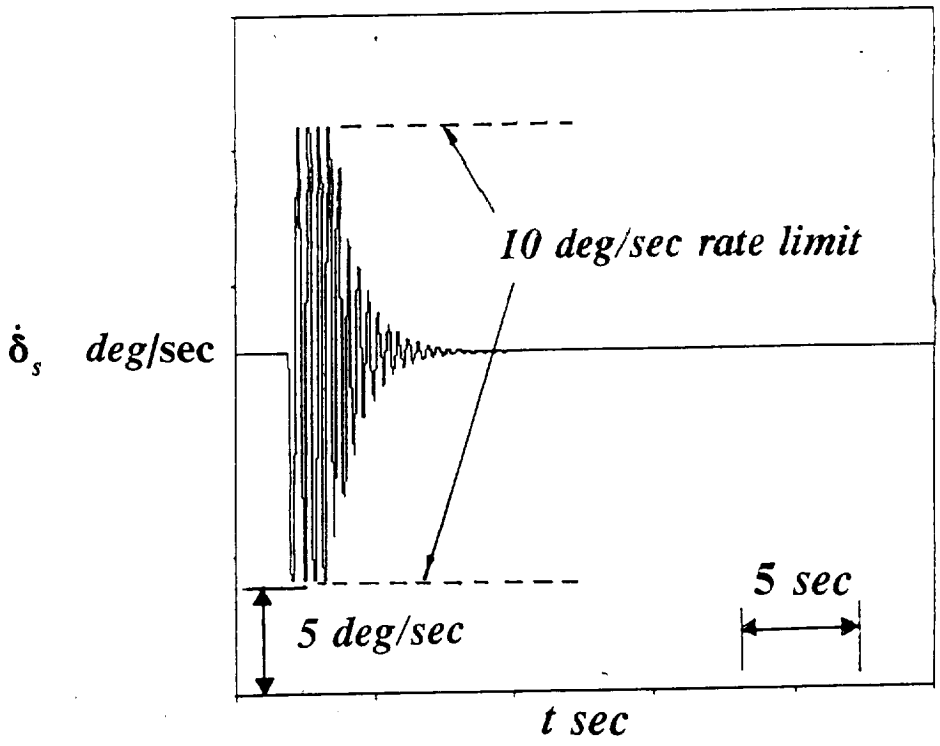

Figure 24 Stabilator rate corresponding to Fig. 23

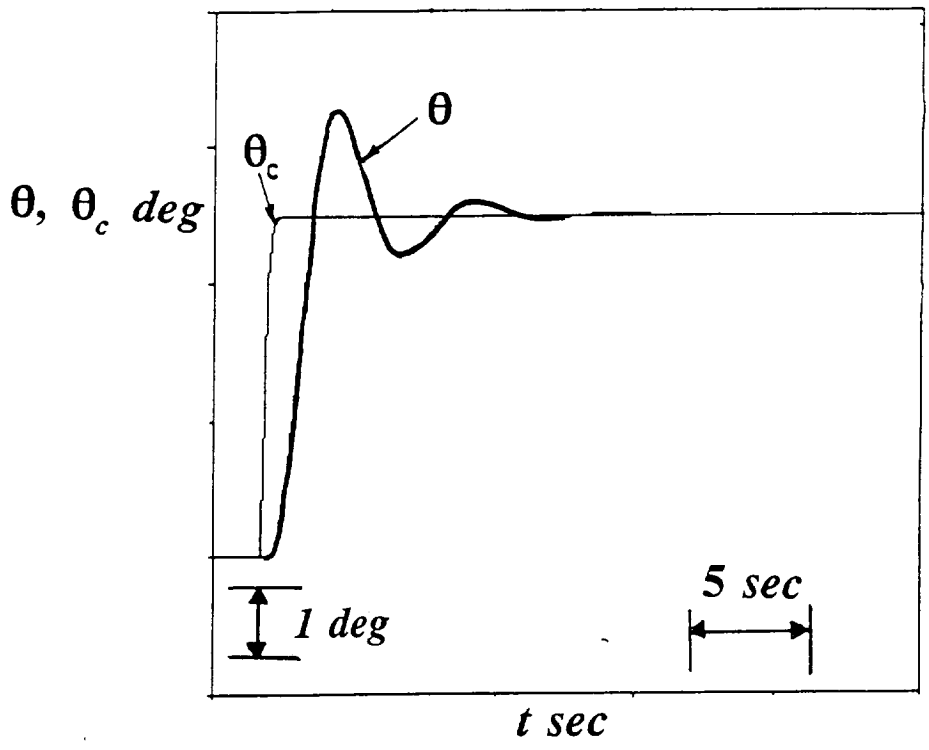

Figure 23 Pilot/vehicle pitch-attitude tracking performance for aircraft damaged as in Fig. 12, with actuator rate limiting of 10 deg/sec, after reconfiguration

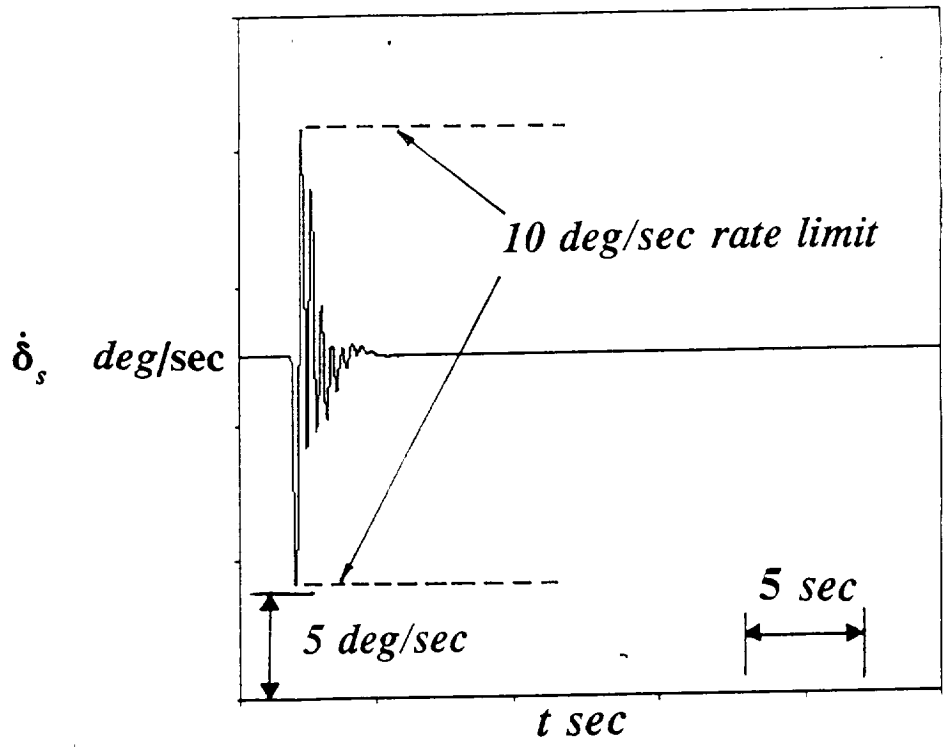

Figure 22 Stabilator rate corresponding to Fig. 21

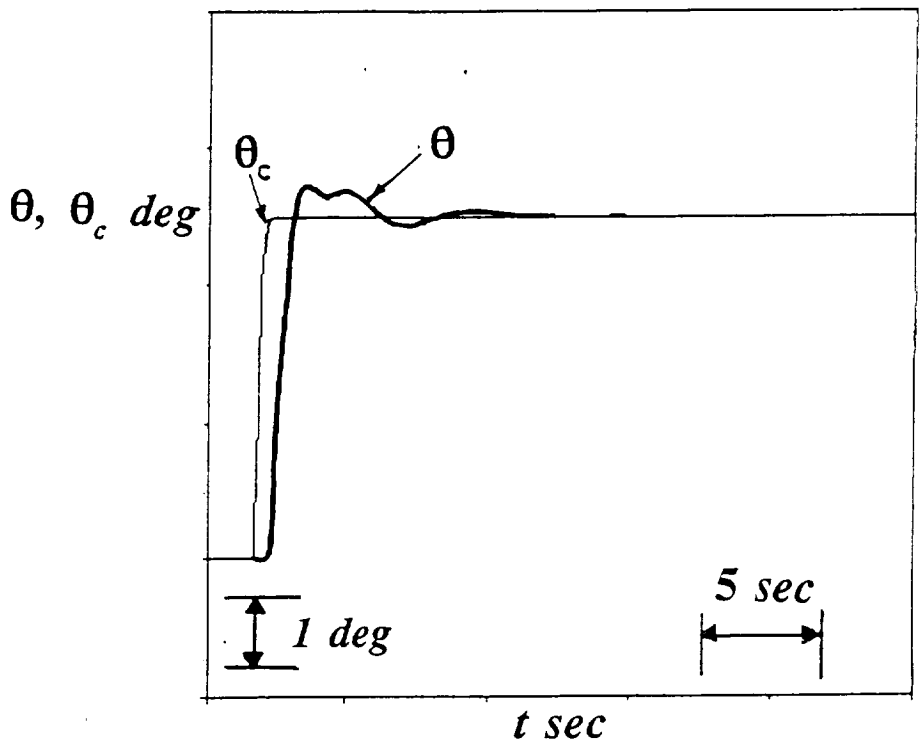

Figure 21 Pilot/vehicle pitch-attitude tracking performance for undamaged aircraft, with actuator rate limiting of 10 deg/sec

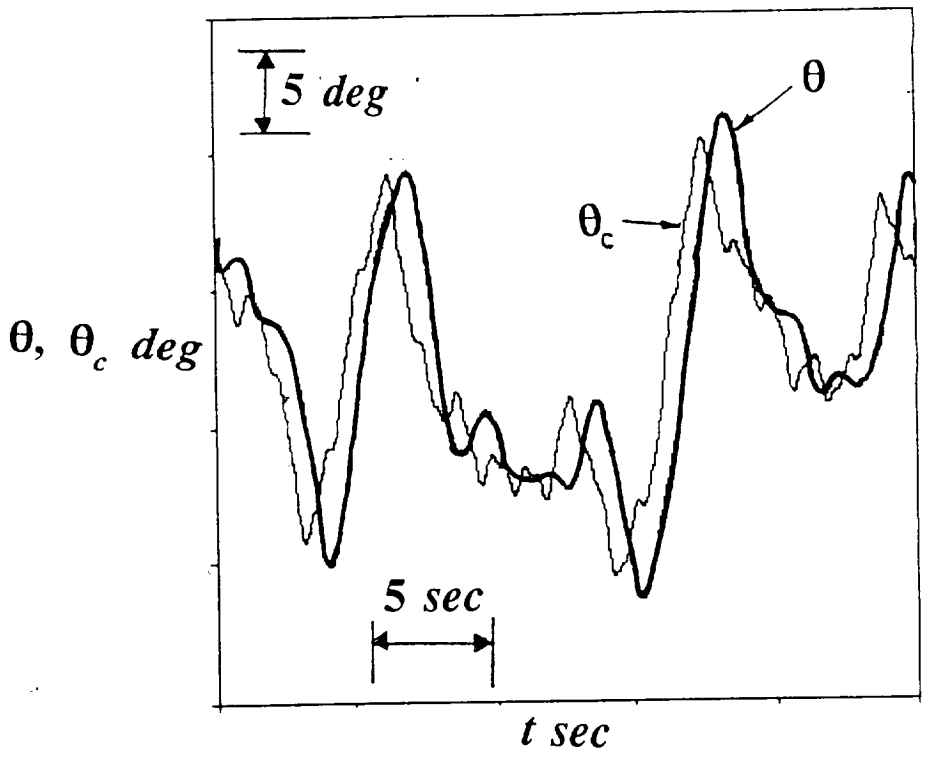

Figure 20 Pilot/vehicle pitch-attitude tracking performance for damage not in modeled set - no reconfiguration required

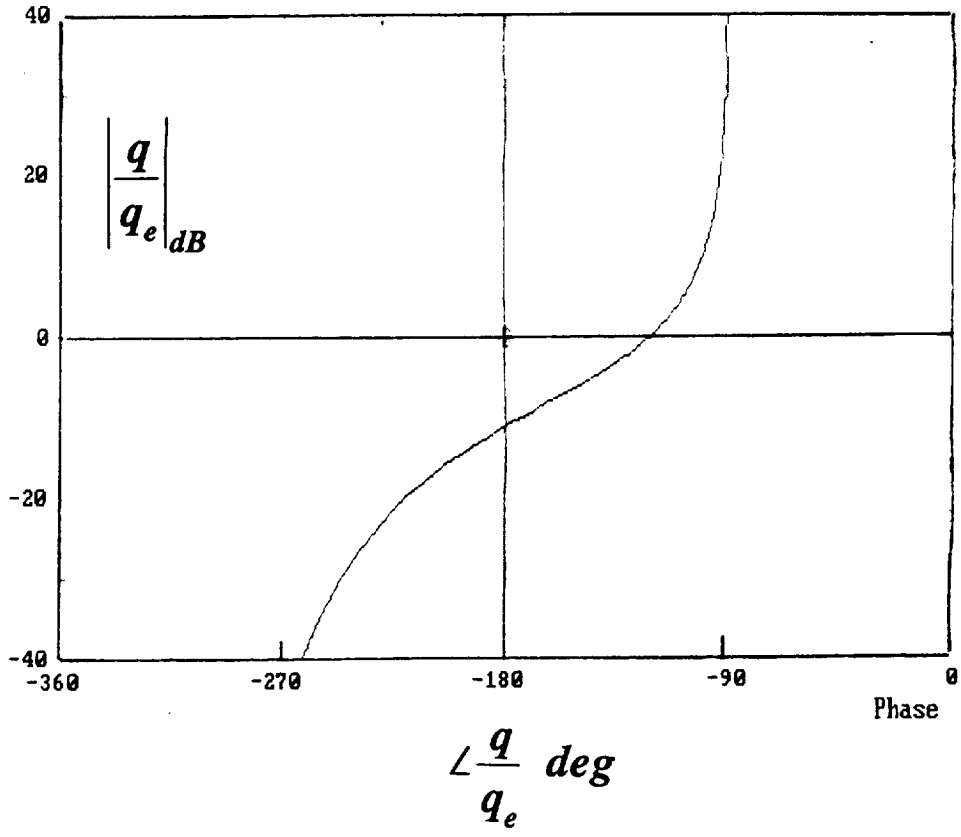

Figure 19 Nichols chart plot of SCAS loop transmission for damaged aircraft not in modeled set

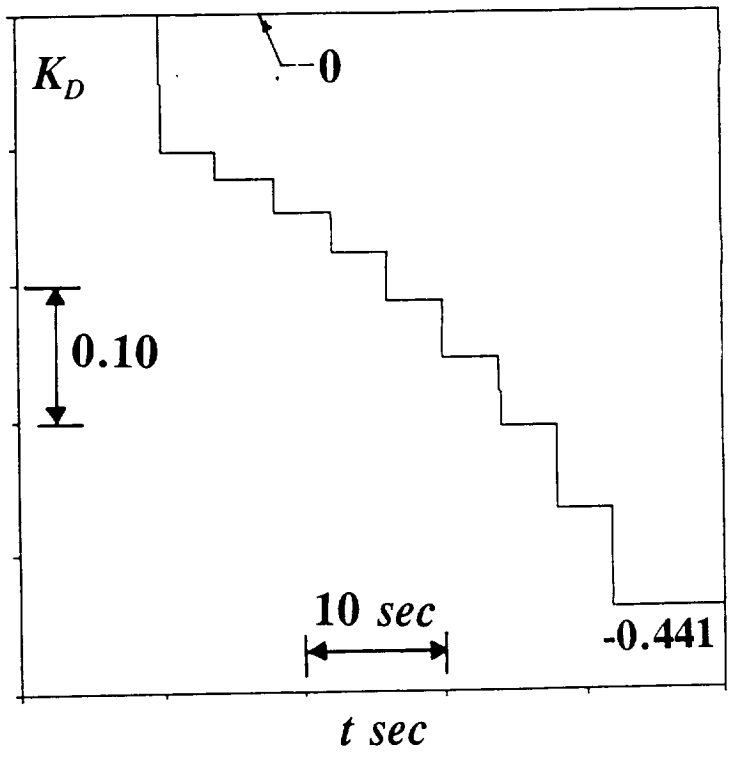

Figure 18 K_D variation during reconfiguration of Fig. 14

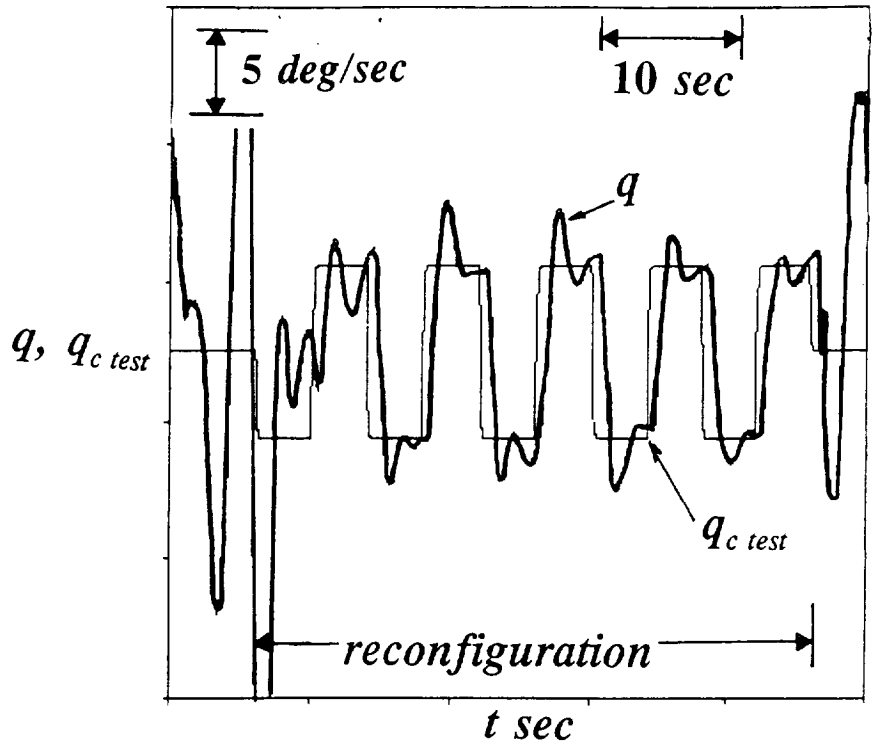

Figure 17 Reconfiguration responses for aircraft damaged as in Fig. 14

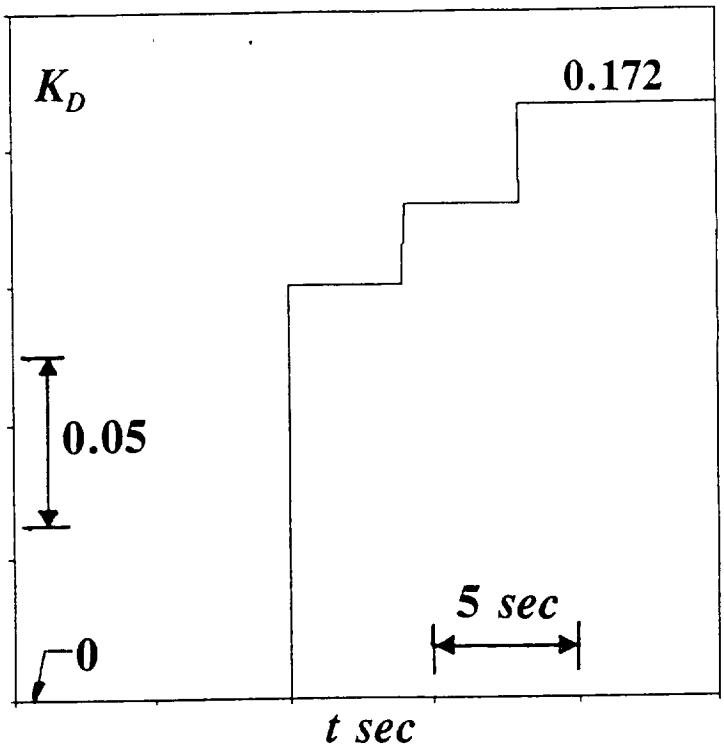

Figure 16 K_D variation during reconfiguration of Fig. 12

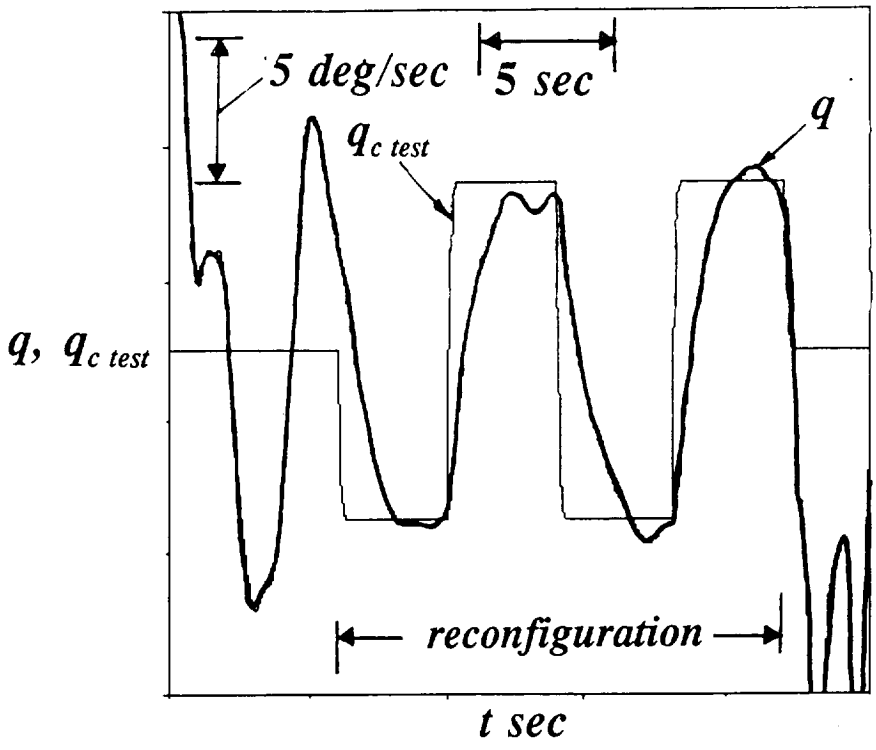

Figure 15 Reconfiguration responses for aircraft damaged as in Fig. 12

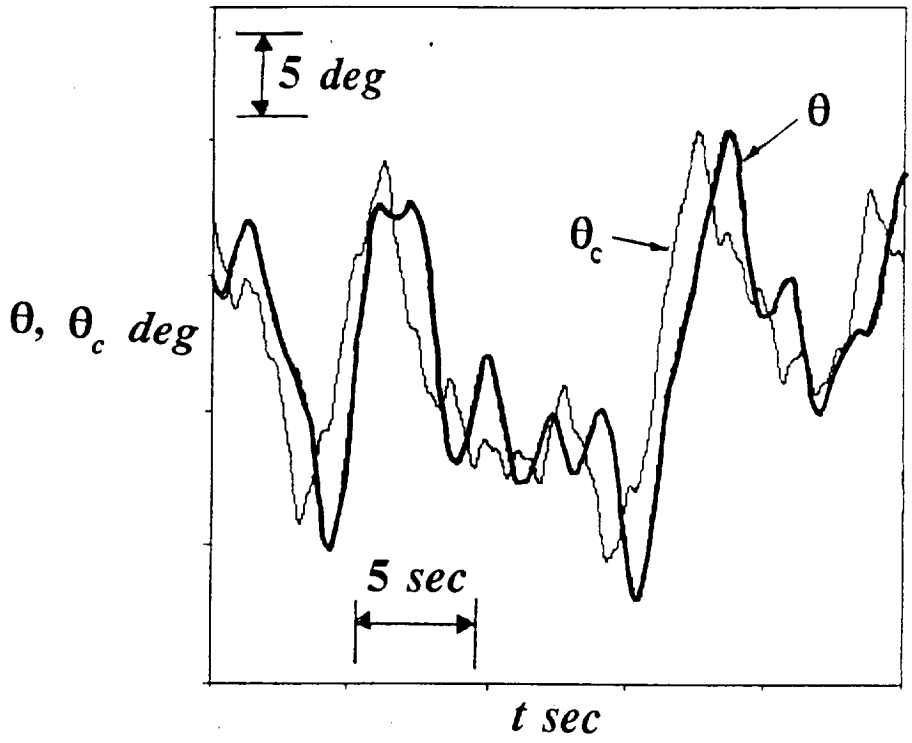

Figure 14 Pilot/vehicle pitch-attitude tracking performance for damaged aircraft after reconfiguration - thrust actuator failed completely, stabilator with added 0.2 sec delay

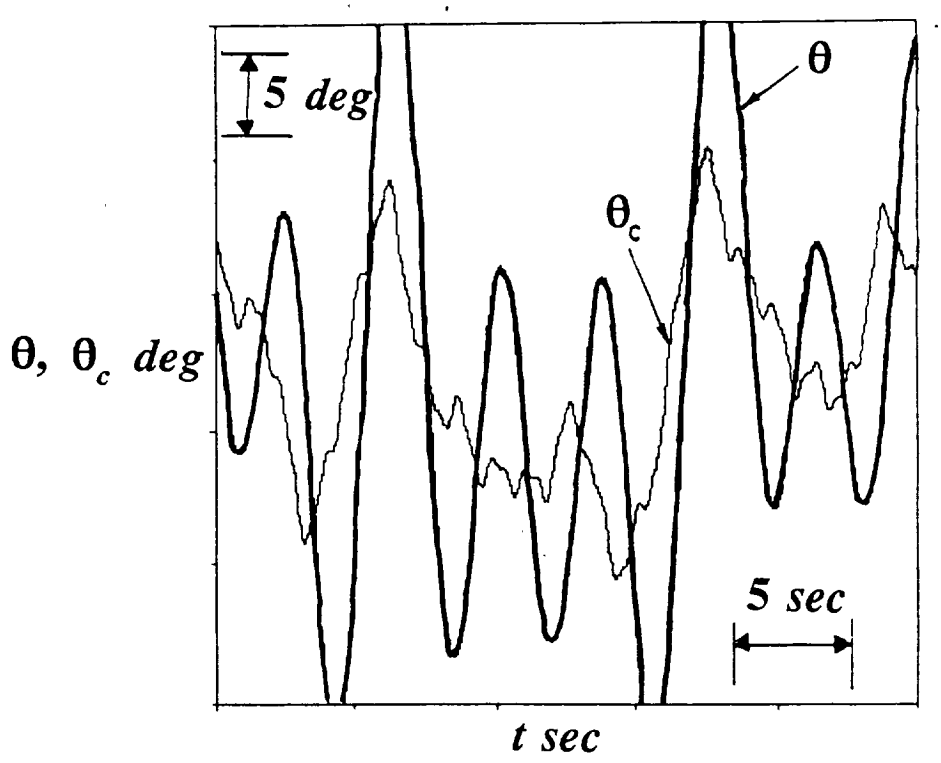

Figure 13 Pilot/vehicle pitch-attitude tracking performance for aircraft damaged as in Fig. 12 but no reconfiguration

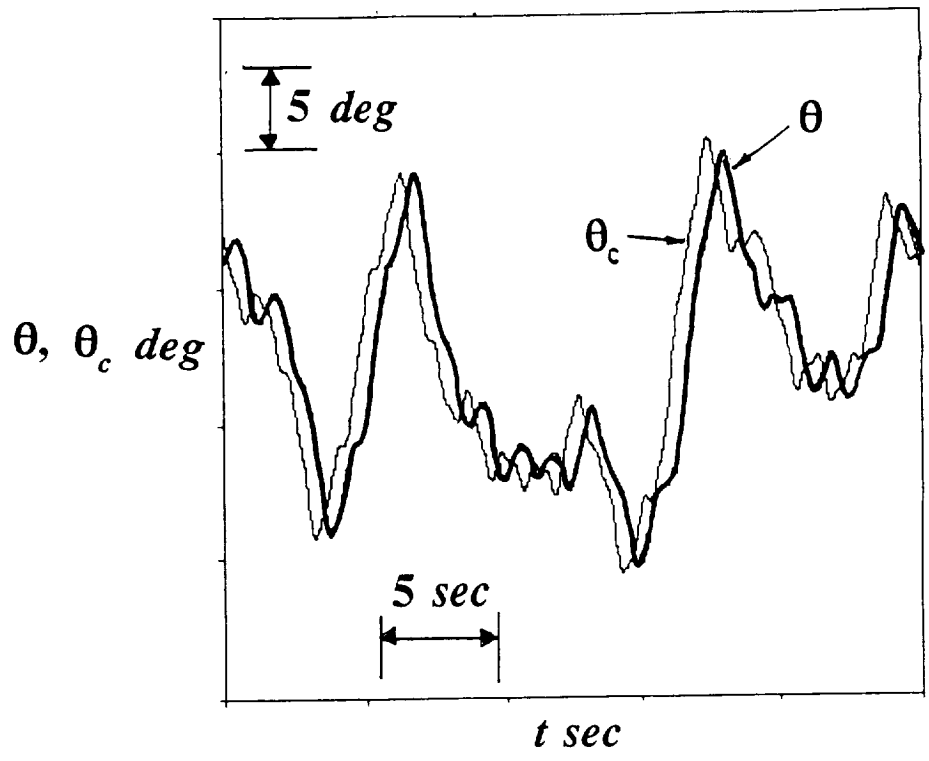

Figure 12 Pilot/vehicle pitch-attitude tracking performance for damaged aircraft after reconfiguration - thrust actuator failed completely, stabilator with 50% effectiveness

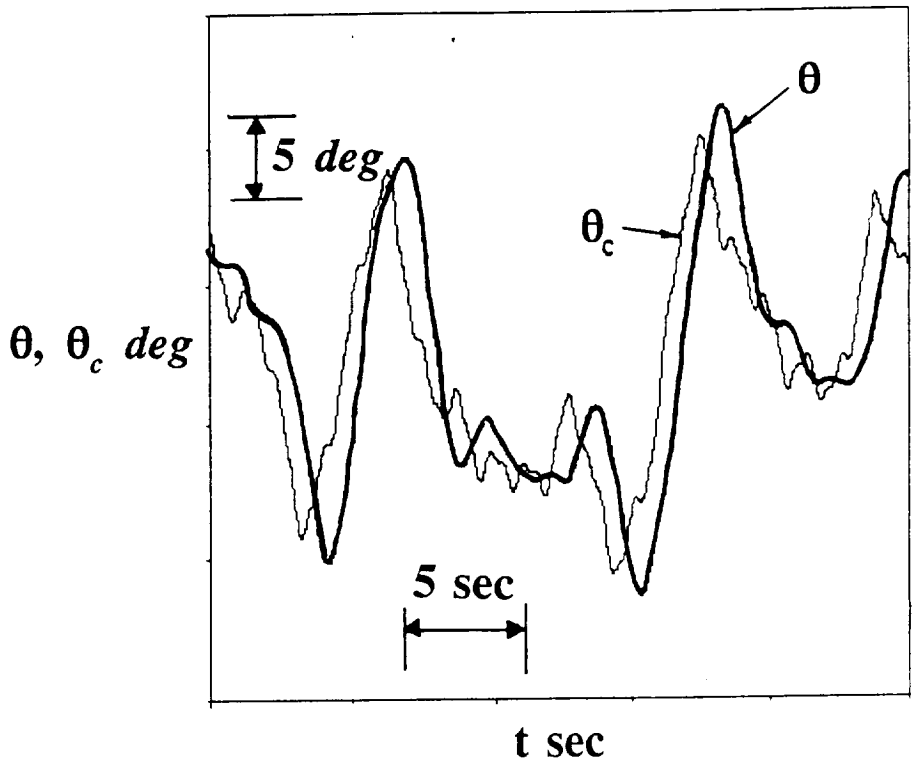

Figure 11 Pilot/vehicle pitch-attitude tracking performance for undamaged aircraft

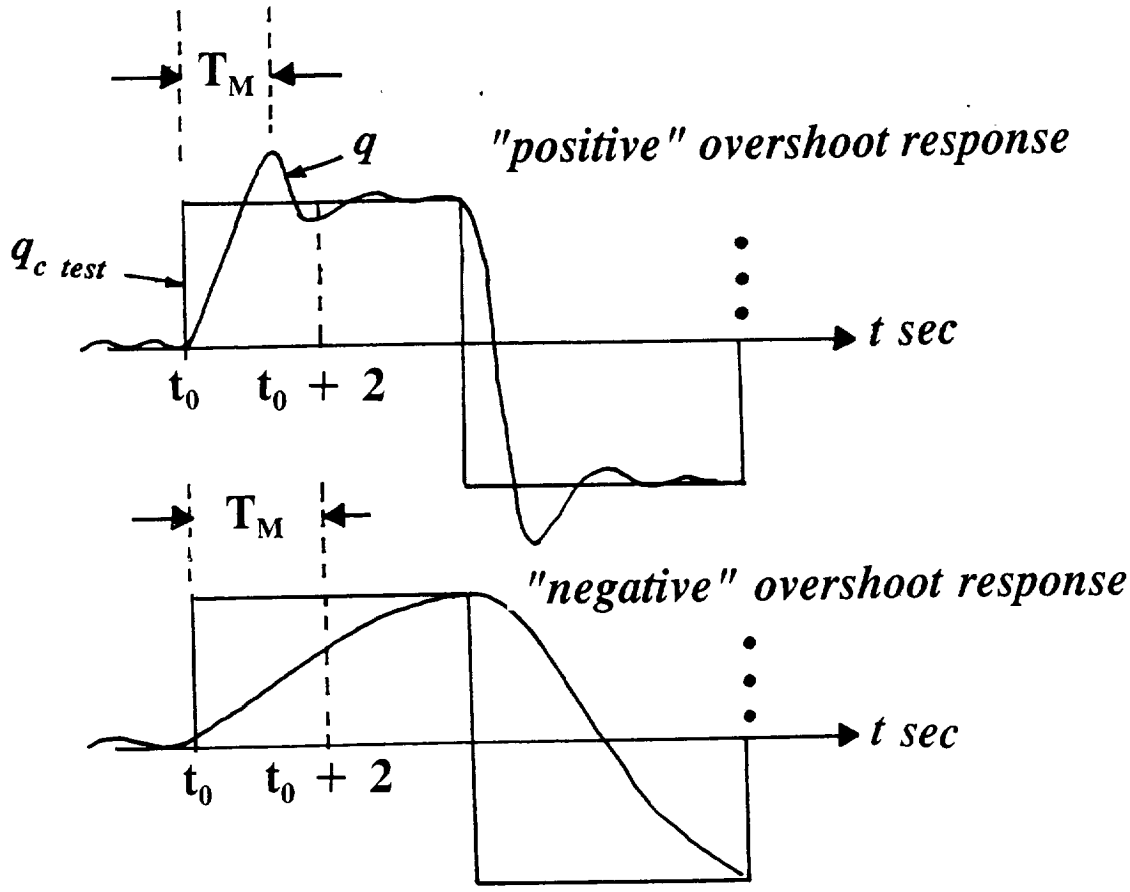

Figure 10 Definition of q-response "effective" time constant

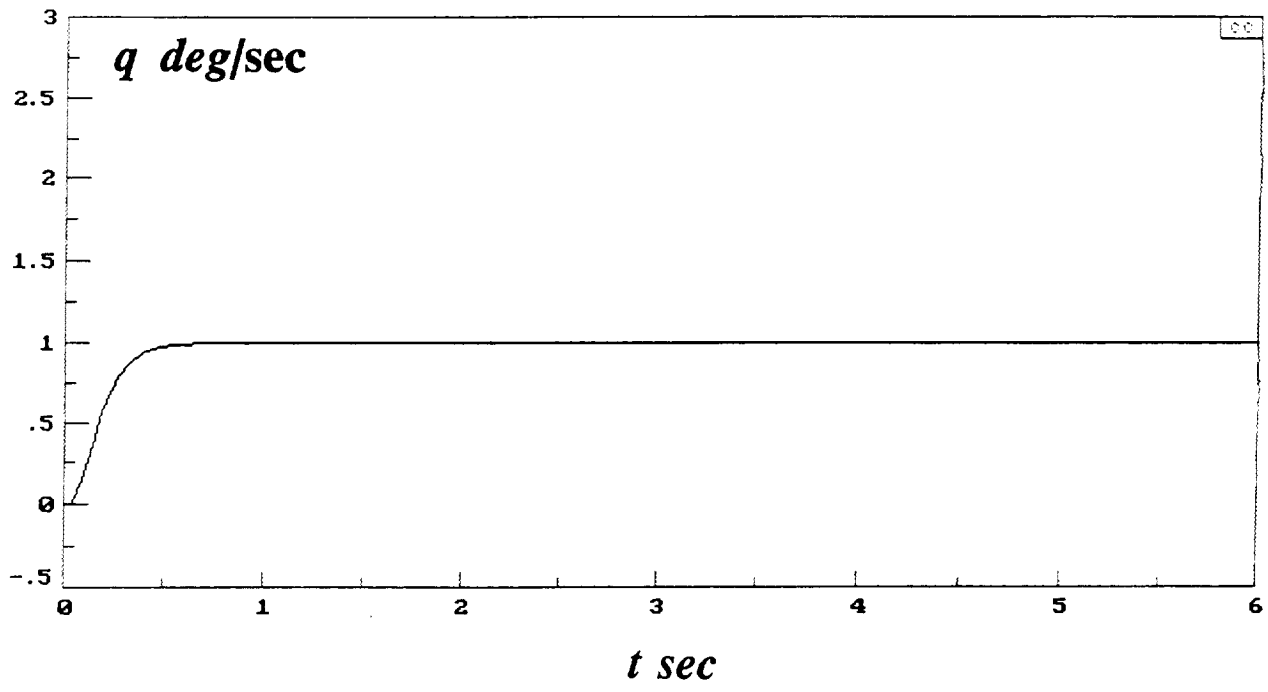

Figure 9 SCAS step response (q to q_{cp}) for undamaged aircraft

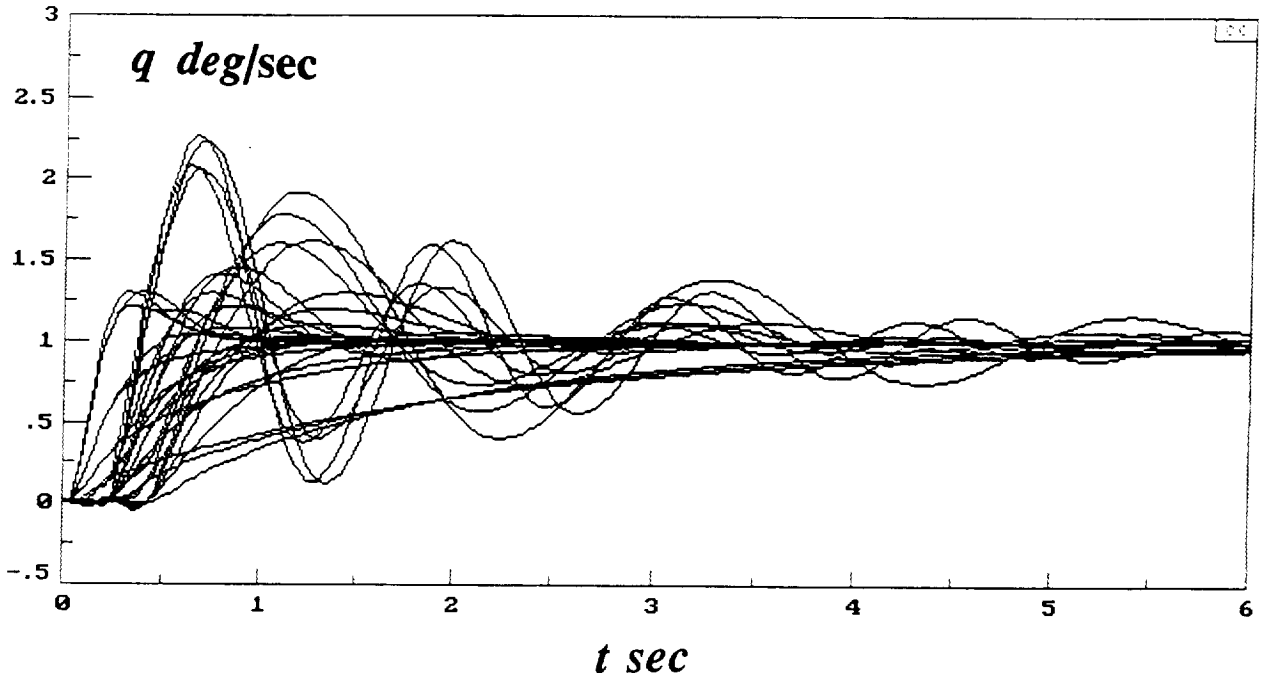

Figure 8 SCAS step responses (q to q_{cp}) for damaged aircraft

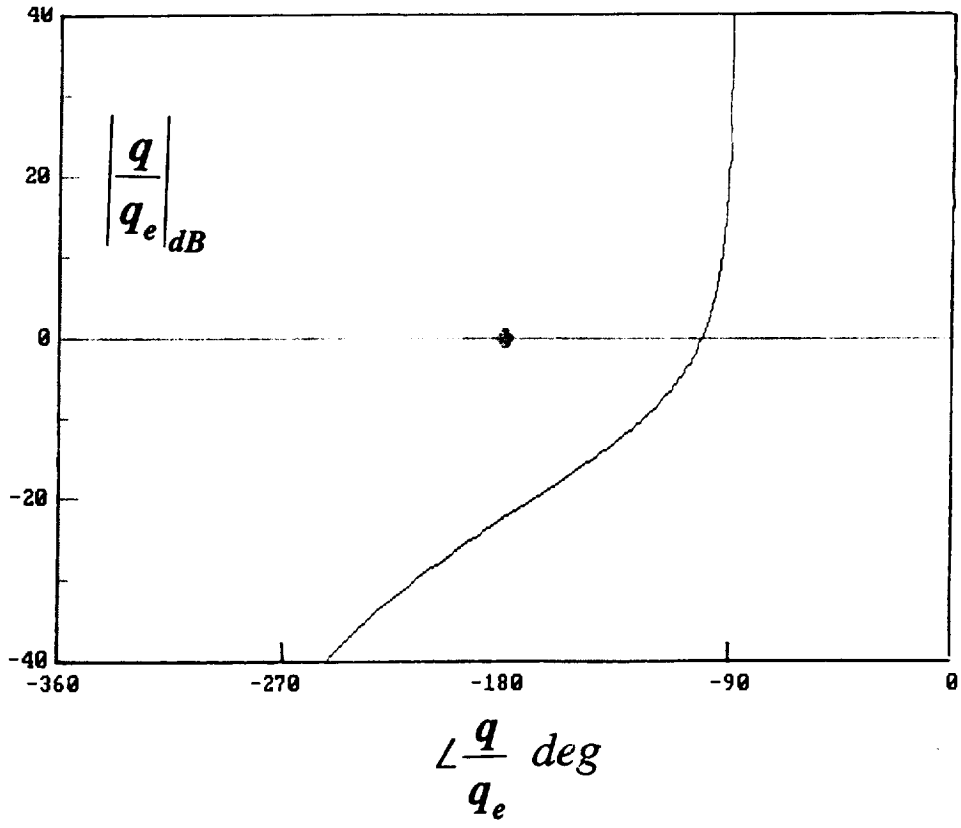

Figure 7 Nichols chart plot of SCAS loop transmission for undamaged aircraft

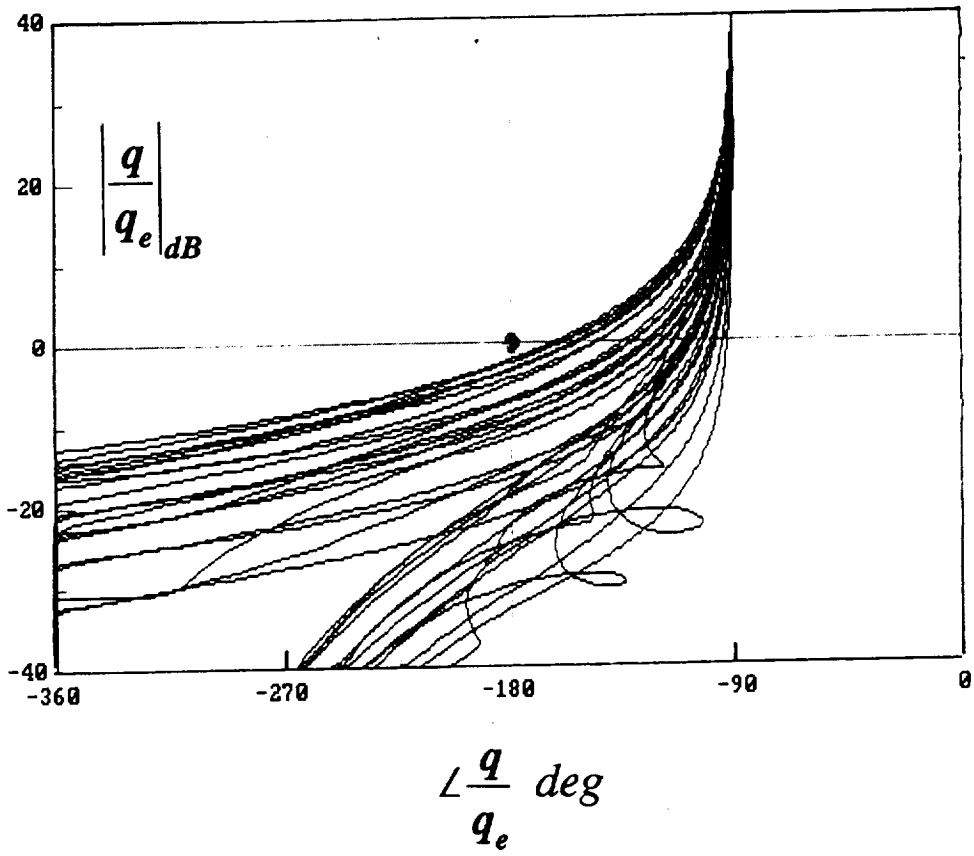

Figure 6 Nichols chart plot of SCAS loop transmissions for damaged aircraft

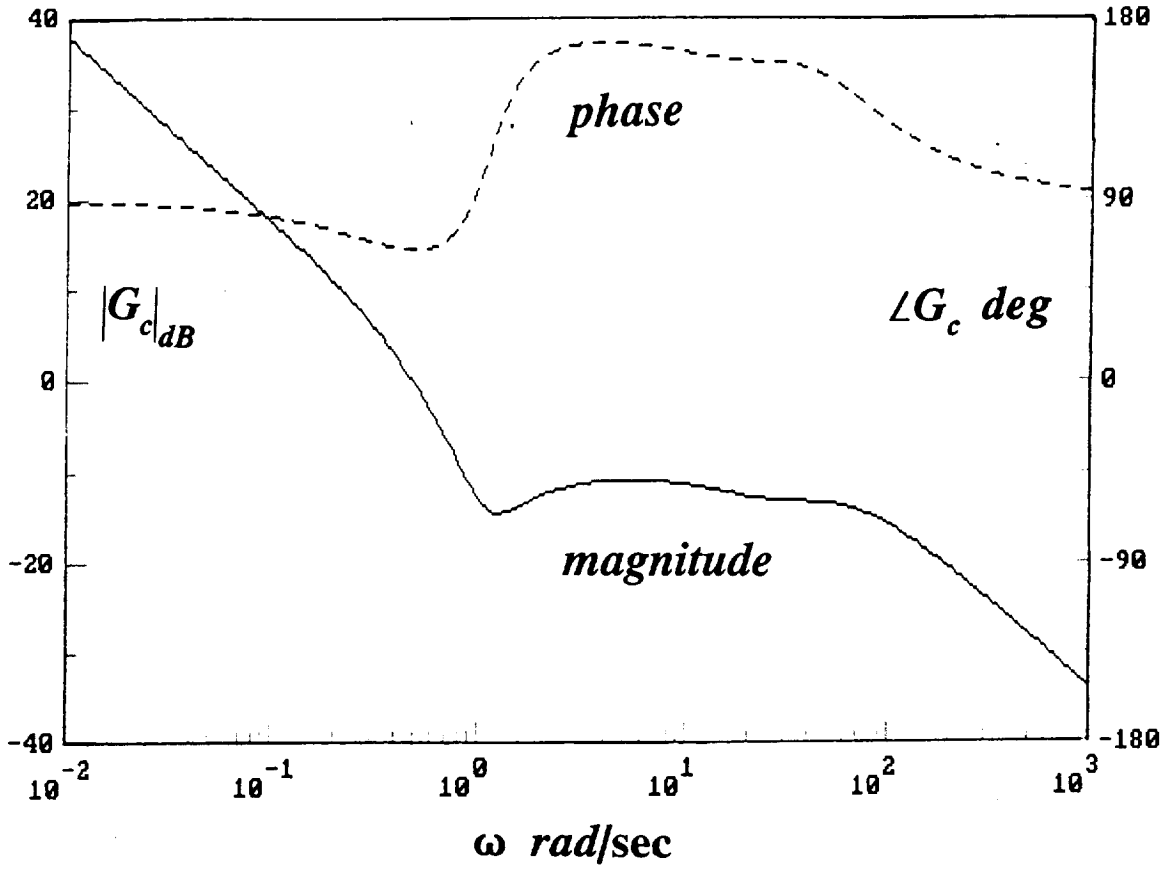

Figure 5 Bode plot of PDT compensator $G_c(s)$

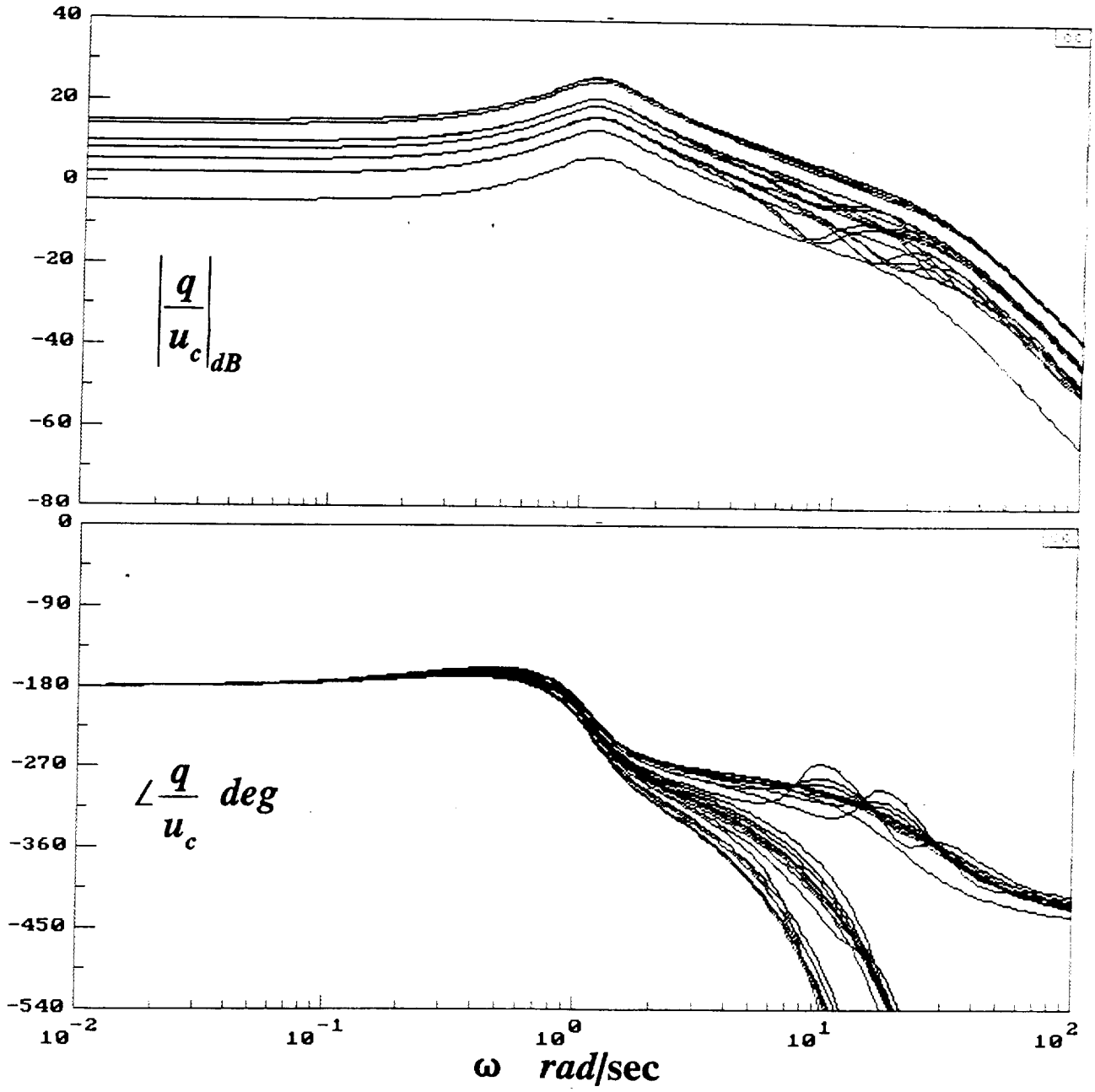

Figure 4 Bode plots of transfer functions of vehicle + actuators with actuator failures

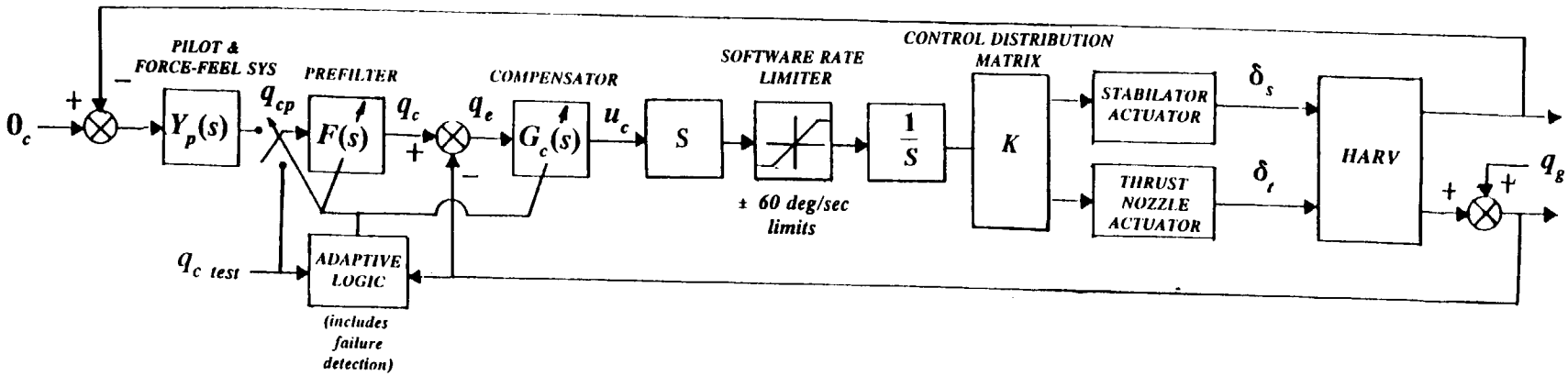

Figure 3 Pitch-rate SCAS and pilot/vehicle control system